Available online at www.sciencedirect.com
SCIENCE DIRECT®
PERGAMON
Polyhedron 21 (2002) 2567–2577
POLYHEDRON
www.elsevier.com/locate/poly

Synthesis, structural characterisation and biological activity of Zn(II) and Pd(II) complexes of 3-substituted 5-(2′-pyridyl)-1,4-benzodiazepin-2-one derivatives

Aleksandar Višnjevac [a,*], Ljerka Tušek-Božić [a], Maja Majerić-Elenkov [a], Zdenko Hameršak [a], Huub Kooijman [b], Erik De Clercq [c], Biserka Kojić-Prodić [a]

[a] 'Rudjer Bošković' Institute, P.O.B. 180, HR-10002 Zagreb, Croatia
[b] Department of Crystal and Structural Chemistry, Bijvoet Center for Biomolecular Research, Utrecht University, Padualaan 8, NL-3584 CH Utrecht, The Netherlands
[c] Rega Institute for Medical Research, Katholieke Universiteit Leuven, B-3000 Leuven, Belgium

Received 29 May 2002; accepted 5 September 2002

Abstract

Zn^{II} and Pd^{II} complexes of 7-bromo-1,3-dihydro-3-hydroxymethyl-1-methyl-5-(2′-pyridyl)-2*H*-1,4-benzodiazepin-2-one ((+)-**L1**), and 3-acetoxymethyl-7-bromo-1,3-dihydro-1-methyl-5-(2′-pyridyl)-2*H*-1,4-benzodiazepin-2-one ((±)-**L2**) were prepared and determined by spectroscopic studies (IR and ^{1}H NMR) and X-ray structure analysis. The influence of the metal coordination on the absolute configuration at the stereogenic centre of the chiral ligands was studied. In Zn**L1**Cl_2 (**1**) a distorted trigonal bipyramid was formed in which **L1** acts as a tridentate *N*,*N*,*O*-ligand, while in the case of Zn**L2**Cl_2 (**3**), Zn^{II} is in a distorted tetrahedral environment coordinated by two azomethine nitrogen and two chlorine atoms. Zn^{II} complexes **1** and **3** are the first zinc complexes of benzodiazepines reported so far. In Pd^{II} complexes **2** and **4**, the expected square-planar coordination was observed. The free ligands and their complexes were evaluated for their in vitro cytostatic activity against the murine L1210/0 and human T-lymphoblast Molt/C8 and CEM/0 cell lines, as well as for their in vitro antiviral activity in different assay systems.

Keywords: Chiral benzodiazepine ligands; Zinc complexes; Palladium complexes; Spectroscopy; X-ray structure analysis; Cytostatic and antiviral activity

1. Introduction

Benzodiazepines are widely used sedative hypnotic compounds [1,2]. After the discovery of benzodiazepine receptors in both the CNS and peripheral tissue in the mid 70s [3–5], it became quite clear that the molecular structure and pharmacological activity of these compounds are closely correlated [6]. Encouraging results of the antiviral and cytostatic assays of some benzodiazepine derivatives have been obtained recently [7–9]. Since coordination with metals can substantially alter the biological activity of organic compounds by modifying their stereochemistry and electronic properties, it is of great importance to study interactions of benzodiazepines with different metals [10,11]. In spite of the huge therapeutic potential of these compounds, very few metal complexes of benzodiazepines with unambiguously determined structures have been reported [12].

On the other hand, chiral 3-substituted benzodiazepine derivatives are the key intermediates in the synthesis of other enantiomerically pure biologically important compounds, like α-amino acids [13]. Therefore, it is of practical interest to study the effect of metal bonding on the absolute configuration at a stereogenic centre of the ligand. In our previous papers, we reported on the use of metal complexes of C(3)-substituted 5-phenyl- and 5-pyridyl-1,4-benzodiazepinones in non-catalytic, catalytic and biocatalytic reactions [14–18]. We also reported copper(II)-promoted racemisation,

* Corresponding author. Tel.: +385-1-457-1203; fax: +385-1-468-0245
E-mail address: aleksandar.visnjevac@irb.hr (A. Višnjevac).

0277-5387/02/$ - see front matter
PII: S0277-5387(02)01251-2

catalytic oxygenation and the ring contraction of 3-substituted 5-(2′-pyridyl)-1,4-benzodiazepin-2-one derivatives [19]. Here we report on the preparation and structural characterisation of the Zn^{II} and Pd^{II} complexes with ligands (+)-**L1** and (±)-**L2** (Scheme 1) as well as on biological properties of free benzodiazepine ligands and their complexes. To our knowledge, compounds Zn**L1**Cl_2 (**1**) and Zn**L2**Cl_2 (**3**) are the first Zn^{II} complexes of benzodiazepines reported so far.

2. Experimental

2.1. Materials and instrumentation

(+)-7-Bromo-1,3-dihydro-3-hydroxymethyl-1-methyl-5-(2′-pyridyl)-2*H*-1,4-benzodiazepin-2-one ((+)-**L1**) was prepared by lipase catalysed kinetic resolution [15] whereas *rac*-3-acetoxymethyl-7-bromo-2,3-dihydro-1-methyl-5-(2′-pyridyl)-2*H*-1,4-benzodiazepin-2-one ((±)-**L2**) was prepared according to the reported method [11]. All other reagents and solvents were analytical grade products and were used without further purification. FTIR spectra were recorded on a Perkin–Elmer 2000 spectrophotometer using KBr (4000–400 cm^{-1}) and polyethylene (400–200 cm^{-1}) pellets. ^1H NMR spectra were performed with a Varian broadband Gemini 300 spectrometer in $CDCl_3$ and DMSO-d_6 containing Me_4Si as an internal standard. Two-dimensional experiments were performed by standard pulse sequences, using Gemini Data System software Version 6.3. Elemental analyses were performed with a Perkin–Elmer Elemental Analyser E-2400 Series 2 (CHN) and thermogravimetric analyses with a Cahn RG electromicrobalance in an air atmosphere.

2.2. Zn[*L1*]Cl_2 (*1*)

A solution of (+)-**L1** (0.072 g, 0.20 mmol) in absolute EtOH (1.0 ml) was added dropwise to a stirred solution of $ZnCl_2 \cdot 2H_2O$ (0.035 g, 0.20 mmol) in absolute EtOH (2.0 ml). The reaction mixture was stirred for 1 h at room temperature (r.t.), the yellow hygroscopic precipitate formed was separated, washed with absolute cold EtOH and stored overnight in vacuum. Yield: 0.031 g (30%). Crystals for X-ray analysis were obtained from absolute EtOH by slow evaporation in a desiccator over silica gel. *Anal*. Calc. for $C_{16}H_{14}BrCl_2N_3O_2Zn \cdot 2H_2O$ (532.53): C, 36.09; H, 3.41; N, 7.89. Found: C, 36.29; H, 3.28; N, 7.32%. IR (cm^{-1} KBr disc): 3369 w br [ν(OH], 1677 vs br [ν(C=O)], 1625 m, 1592 s and 1560 w [δ(OH), ν(C=N), ν(C=C)], 1496 s, 1485 s, 1444 m, 1403 m, 1337 s, 1300 sh, 1265 sh, 1253 m, 1190 w, 1125 m-s, 1102 m, 1050 w, 1020 m, 978 w, 889 w, 834 m-s, 801 m-s, 756 w, 724 w, 678 m and 642 w-m; IR (cm^{-1}, polyethylene): 314 m-s br.

2.3. Pd[*L1*]Cl_2 (*2*)

A solution of (+)-**L1** (0.053 g, 0.15 mmol) in MeOH (1.0 ml) was added dropwise to a stirred solution of $Na_2PdCl_4 \cdot 3H_2O$ (0.055 g, 0.15 mmol) in MeOH (3.0 ml). The reaction mixture was stirred for 2 h at r.t., the yellow precipitate formed was filtered off, washed with cold MeOH and dried in vacuum over P_2O_5. Yield: 0.070 g (87%). Single crystals were obtained from DMF.

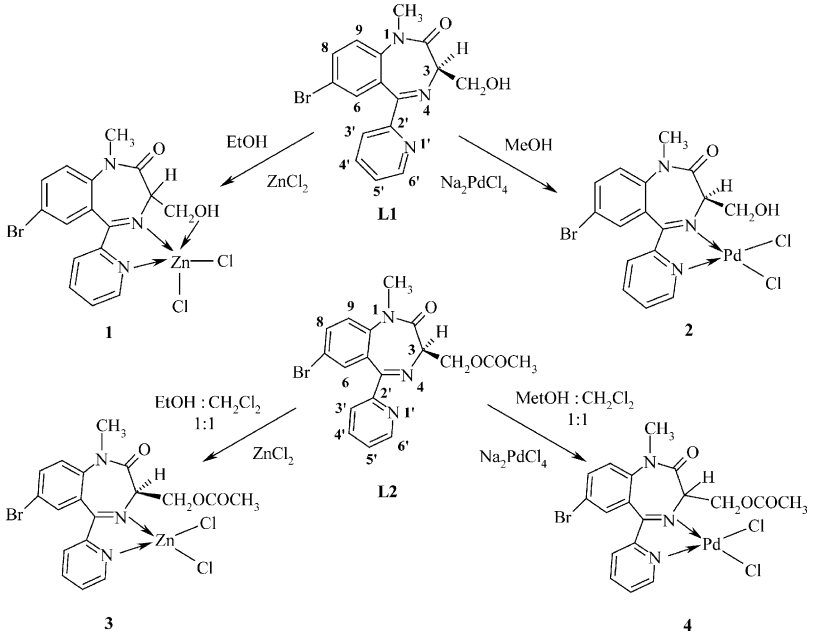

Scheme 1. Chemical diagrams of ligands and complexes.

Anal. Calc. for $C_{16}H_{14}BrCl_2N_3O_2Pd$ (537.73): C, 35.80; H, 2.44; N, 7.87. Found: C, 36.17; H, 2.75; N, 7.61%. IR (cm^{-1} KBr disc): 3427 m-s [ν(OH)], 1669 vs [ν(C=O)], 1590 s, 1561 m and 1541 w [δ(OH), ν(C=N), ν(C=C)], 1489 s, 1479 s, 1442 m, 1443 w, 1400 m, 1352 m, 1321 m-s, 1255 m-s, 1187 w, 1140 w-m, 1125 w, 1068 m, 1034 m-s, 97 w, 924 w, 889 w, 826 s, 791 m, 751 w-m, 745 w-m, 677 w-m and 659 w; IR (cm^{-1}, polyethylene): 373 w, 345 w, 328 w-m and 299 w.

2.4. *Zn[**L2**]Cl$_2$ (**3**)*

A solution of **L2** (0.100 g, 0.25 mmol) in a 1:1 mixture of absolute EtOH and CH_2Cl_2 (2 ml) was added dropwise to a stirred solution of $ZnCl_2 \cdot 2H_2O$ (0.050 g, 0.29 mmol) in the same mixture of solvents (2 ml). After complete addition, the reaction mixture was continuously stirred for 24 h at ambient temperature and left at 277 K for another 48 h. Yellow crystals were obtained (yield: 0.070 g, 52%). *Anal.* Calc. for $C_{18}H_{16}BrCl_2N_3O_3Zn \cdot H_2O$ (556.77): C, 38.82; H 3.26; N 7.58. Found: C, 39.28; H, 3.12; N, 7.15%. IR (cm^{-1} KBr disc): 3508 w br [ν(OH)], 1742 vs [ν(C=O) acetate], 1691 vs br [ν(C=O) lactam, ν_{as}(COO)], 1599 m, 1589 s, 1568 m and 1556 s [δ(OH),ν(C=N), ν(C=C)], 1480 s, 1470 s, 1439 s, 1427 m, 1395 m-s, 1364 m-s, 1334 s, 1301 m, 1261 s, 1221 vs br, 1186 m, 1125 m, 1120 m, 1102 s, 1054 m, 1023 s, 973 w, 932 w-m, 920 w-m, 892 w, 830 s, 802 s, 745 m-s, 720 w-m, 710 w, 678 s, 643 m and 619 w; IR (cm^{-1}, polyethylene): 335 s br, 313 m-s and 326 w br.

2.5. *Pd[**L2**]Cl$_2$ (**4**)*

A mixture of **L2** (0.100 g, 0.25 mmol) and $Na_2[PdCl_4] \cdot 3H_2O$ (0.084 g, 0.25 mmol) in a 1:1 mixture of MeOH and CH_2Cl_2 (3.0 ml) was stirred for 3 h at ambient temperature. The yellow precipitate formed was filtered off, washed with cold MeOH and CH_2Cl_2, and dried in vacuum over P_2O_5. Yield: 0.120 g (80%). *Anal*. Calc. for $C_{18}H_{16}BrCl_2N_3O_3Pd$ (579.77): C, 37.28; H, 2.78; N, 7.28. Found: C, 36.81; H, 3.00; N, 6.71%; IR (cm^{-1} KBr disc): 1742 s [ν(C=O) acetate], 1683 vs and 1668 vs [ν(C=O) lactam, ν_{as}(COO)], 1593 m, 1564 w and 1539 w [ν(C=N), ν(C=C)], 1489 m, 1472 m, 1441 w, 1403 w, 1368 w-m, 1340 m, 1257 s, 1247 m-s, 1214 s, 1190 w, 1126 w, 1105 w-m, 1040 sh, 1034 m-s, 980 w, 920 w, 874 w, 842 w, 822 w, 798 w, 760 w, 709 w, 679 w, 642 w and 616 w-m; IR (cm^{-1}, polyethylene): 353 m-s, 343 m, 328 m, 313 m and 280 w-m.

2.6. *X-ray structure analysis*

Suitable single crystals were obtained by a slow evaporation from different solvents listed in Table 1, which also summarises crystal data, experimental details of data collection and refinement. Data were collected on an Enraf–Nonius CAD4 diffractometer for complex **3**, and on a Nonius Kappa CCD 2000 diffractometer for **1** and **2**. Data were corrected for Lp effects [20]. Structures of **1** and **3** were solved using the package SIR-97 [21], whereas the structure of **2** was solved with SHELXS-86 [22]. Complex **2** was refined with a racemic twin model. The occupation of the component with opposite chirality from that shown in Fig. 2 refined to 0.007(9), indicating that the crystal is enantiopure and has strong inversion distinguishing power [23]. All data were refined using the package SHELXL-97 [24]. Molecular geometry calculations and illustrations were prepared with PLATON [25]. Atomic scattering factors were those included in SHELXL-97. The H-atom coordinates were calculated geometrically and refined using the SHELXL-97 riding model.

2.7. *In vitro cytostatic assays*

The cytostatic activity of the free benzodiazepine ligands and their metal complexes was assayed in vitro on the murine leukemia L1210/0 cell line as well as on the human T-lymphoblast Molt4/C8 and CEM/0 cell lines, according to previously described methods [26,27]. The activity was expressed as the concentration (in μg ml^{-1}) of the compound at which tumour cell growth showed 50% inhibition (IC_{50}).

2.8. *In vitro antiviral assays*

The antiviral and cytotoxicity assays of compounds were carried out in either Vero, HEL or HeLa cell cultures, following previously established procedures [28]. The inhibitory effects of the test compounds on the replication of parainfluenza-3 virus, reovirus type 1, Sindbis virus, Coxsackie virus B4 and Punta Toro virus was evaluated in Vero cells, on herpes simplex virus type 1 (KOS), herpes simplex virus type 2(G), vaccinia virus, vesicular stomatitis virus and herpes simplex virus type 1 (TK^- KOS ACV) in HEL cells, and on vesicular stomatitis, Coxsackie virus B4 and respiratory syncytial virus in HeLa cells. The antiviral activity was expressed as concentration of the compound required to reduce virus-induced cytopathogenicity by 50%.

3. Results and discussion

3.1. *Preparation of the complexes*

The reaction of benzodiazepine ligands **L1** and **L2** with the appropriate zinc and palladium salt yielded dichloro adducts as depicted in Scheme 1. The enantiomerically pure (+)-**L1** gave with $ZnCl_2$ in absolute ethanol the pale yellow complex dichloro-[7-bromo-1,3-dihydro-3-hydroxymethyl-1-methyl-5-(2′-pyridyl)-2*H*-

Table 1
Crystallographic data, crystallisation details, structure solution and refinement of compounds **1**, **2** and **3**

Compound	**1**	**2**	**3**
Empirical formula	$C_{16}H_{14}BrCl_2N_3O_2Zn\cdot CH_3CH_2OH$	$C_{16}H_{14}BrCl_2N_3O_2Pd\cdot C_3H_7NO$	$C_{18}H_{16}BrCl_2N_3O_3Zn$
M_r	496.50	610.62	538.53
Temperature during data collection (K)	293(2)	150	293(2)
Wavelength (Å)	1.54183	0.71073	0.71073
Crystal system	Monoclinic	orthorhombic	orthorhombic
Space group	$P2_1/n$	$P2_12_12_1$	$P2_12_12_1$
a (Å)	9.894(1)	7.1411(10)	10.008(2)
b (Å)	12.709(2)	17.081(4)	10.859(3)
c (Å)	16.747(5)	18.161(5)	37.998(7)
β (°)	90.703(1)		
V (Å^3)	2105.6(7)	2215.2(9)	4128(3)
Z	4	4	8
D_{calc} (Mg m^{-3})	1.712	1.831	1.7325
Crystallisation solvent(s)	Ethanol	DMF, DMSO	ethanol, dichloromethane
Crystal colour	Colourless	yellow	yellow
Absorption correction	None	none	Ψ-scan
Θ_{max}	36.2	27.4	26.3
Index ranges	$-8 \le h \le 8$, $-10 \le k \le 10$, $-13 \le l \le 13$	$-9 \le h \le 9$, $-22 \le k \le 22$, $-23 \le l \le 23$	$-12 \le h \le 0$, $0 \le k \le 13$, $0 \le l \le 47$
Total data collected	1905	47 954	4754
Unique data	969	5052	4721
Observed data $[(I > 2\sigma(I)]$	814	3640	1643
R_1 $[F_o > 4\sigma(F_o)]$	0.0771	0.0416	0.0892
wR_2 (F^2)	0.2295	0.0623	0.2834
S	1.089	1.022	1.206
Parameters	195	278	289
$\Delta\rho_{max}$, $\Delta\rho_{min}$ (e Å^{-3})	0.84, −0.56	0.50, −0.52	1.23, −1.71

1,4-benzodiazepin-2-one-*N*,*N*,*O*]zinc(II) (**1**). The reaction of 60% enantiomerically pure **L2** [19] and $ZnCl_2$ in a 1:1 mixture of ethanol and dichloromethane yielded the enantiomerically pure complex dichloro-[3-acetoxymethyl-7-bromo-1,3-dihydro-1-methyl-5-(2′-pyridyl)-2*H*-1,4-benzodiazepin-2-one-*N*,*N*]zinc(II) (**3**), which reversibly changes its colour from pale-yellow to pink. In the mother liquor, crystals are yellow-coloured, whereas exposed to air they quickly change their colour to pink. Hygroscopic properties of the compound might be related to this effect. The reaction of benzodiazepine ligands with Na_2PdCl_4 in methanol (**L1**) and in a mixture of methanol and dichloromethane 1:1 (**L2**), yielded the yellow square-planar complex *cis*-dichloro-[7-bromo-1,3-dihydro-3-hydroxymethyl-1-methyl-5-(2′-pyridyl)-2*H*-1,4-benzodiazepin-2-one-*N*,*N*]palladium(II) (**2**) and *cis*-dichloro-[7-bromo-1,3-dihydro-3-acetoxymethyl-1-methyl-5-(2′-pyridyl)-2*H*-1,4-benzodiazepin-2-one-*N*,*N*]palladium(II) (**4**), respectively. No racemisation was observed during the formation of the Pd^{II} complexes.

3.2. The crystal structures

ORTEP [29] drawings of **1** and **2** are given in Figs. 1 and 2, respectively. A PLUTON drawing of the molecular structure of **3** is given in Fig. 3. The crystal structure of **2** is depicted in Fig. 4. The selected geometry for all structures is summarised in Tables 2 and 3. Hydrogen bonds are listed in Table 4.

In the molecular structure of **1**, Zn^{II} is five-coordinated. **L1** acts as a tridentate ligand, through two azomethine nitrogens, N4 and N15, and hydroxy oxygen O13 (Fig. 1). Fivefold coordination of Zn^{II} is completed with two chlorine atoms. Bond distances Zn–O and Zn–N (Table 3) are in accordance with the previously reported values for five-coordinated Zn^{II} complexes found in the *CSD* [30]. The molecule of **1** displays a strongly distorted trigonal bipyramidal coordination, with Cl1, Cl2 and N4 in an equatorial plane, whereas the Zn atom is slightly above it [0.045(2) Å]. The distortion from the regular trigonal bipyramidal coordination has been introduced by the angle N15–Zn–O13 of 145.8(5)° (that differs considerably from the required 180°). Molecular structure of **1** exhibits the usual *boat* conformation [31]. There are no significant differences in values of geometrical parameters inside the diazepin ring of complex **1** (Table 2) and its Cu^{II} analogue described in our previous paper [19]. Thus, the metal coordination has a minor influence on the conformation of the diazepine ring. In **2**, Pd^{II} is, as expected, in a fourfold square-planar coordination

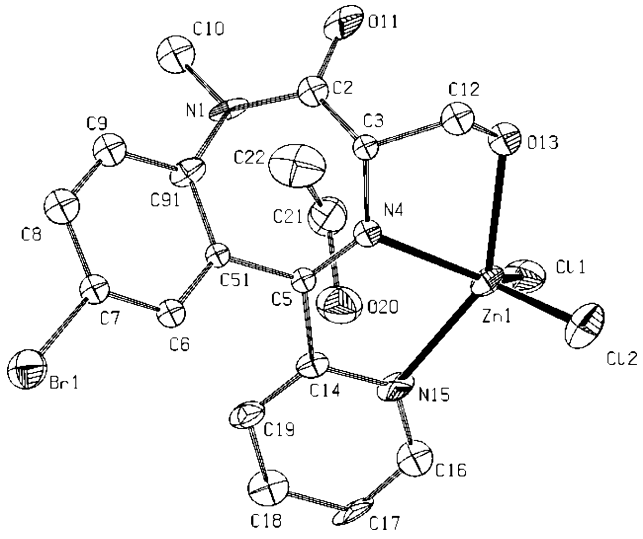

Fig. 1. ORTEP drawing of complex **1** with atom numbering. Thermal ellipsoids are scaled at the 30% probability level. Hydrogen atoms are omitted for clarity.

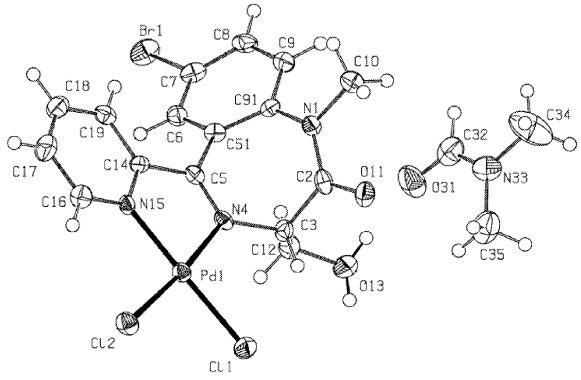

Fig. 2. ORTEP drawing of complex **2** with atom numbering. Thermal ellipsoids are scaled at the 50% probability level.

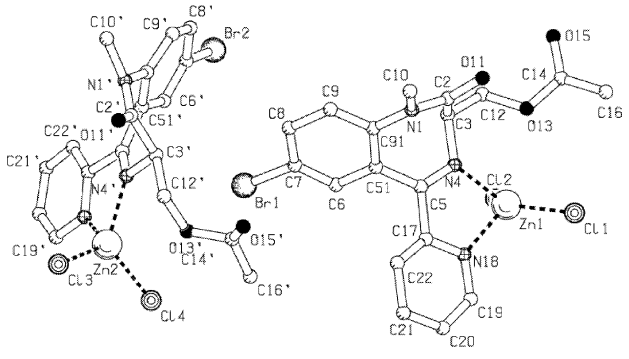

Fig. 3. PLUTON drawing of complex **3**. Hydrogen atoms are omitted for clarity.

[deviations from the least-squares plane ranging from −0.038(4) Å for N15 to 0.0300(14) Å for Cl2] (Fig. 2). In this complex, **L1** acts as a bidentate ligand to Pd^{II} through the pyridine and diazepine nitrogens. The fourfold coordination is completed by two chlorine

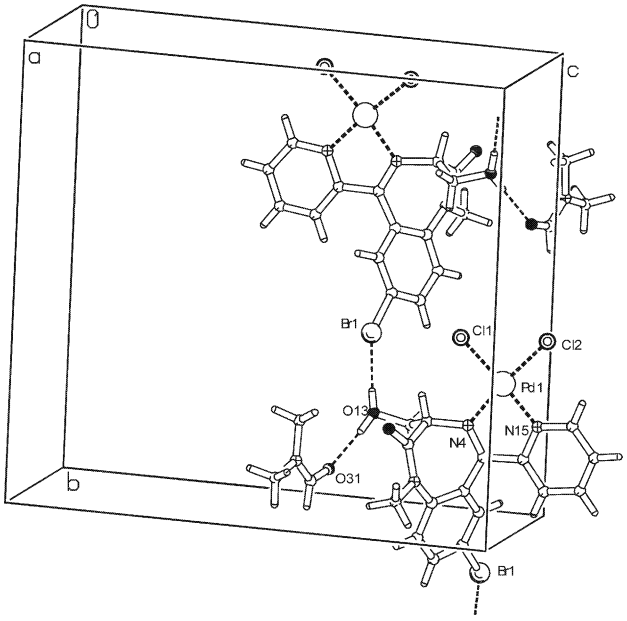

Fig. 4. Crystal packing of the complex **2**. The complex molecules are connected via an O13–H···Br interaction. This interaction has half site occupancy, the other half being occupied by an O13–H···O31 hydrogen bond which connects the complex molecule with a solvent.

atoms. X-ray structure analysis has revealed *S*-configuration at the C3 stereogenic centre. Significant conformational changes in the ligand upon coordination were not observed; hence the *boat* conformation of the seven-membered diazepine ring is retained. In **3**, **L2** acts as an *N*,*N*-bidentate ligand chelating Zn^{II} through diazepine and pyridyl nitrogen atoms (Fig. 3). The fourfold coordination is completed by two chlorine atoms. Severely distorted tetrahedra were observed; bond angles involving Zn^{II} ranged from 79.1(7)° to 125.3(5)° in molecule **A**, and from 76.5(8)° to 119.9(6)° in molecule **B** (Table 3). Unlike in **1**, hydroxy oxygen O13 is not coordinated to Zn^{II}. Complex **3** crystallises in the non-centrosymmetric space group $P2_12_12_1$ with two independent molecules in an asymmetric unit. The *R*-absolute configuration at the stereogenic centres C3 and C3′ was determined by X-ray structure analysis. Comparison of the coordination details in Cu^{II} complexes of **L1** and **L2**, and in their Zn^{II} analogues, reveals significant differences, related to their electronic configuration [32]. Both Cu^{II} and Zn^{II} form with **L1** five-coordinated complexes, and **L1** acts as an *N*,*N*,*O*-tridentate ligand. In **L2**, instead of an hydroxymethyl group at C3, there is a bulky acetoxymethyl group, and for steric reasons O13 is not involved in the metal coordination. Therefore, copper forms five-coordinated species using lactame oxygen from the neighbouring molecule to complete the fivefold coordination in the shape of square-planar pyramide with a long apical Cu^{II}–O bond, whereas Zn^{II} retains the fourfold coordination sphere [22]. However, in the active sites of zinc-

Table 2
Selected bond lengths (Å), angles (°) and torsion angles (°) in **L2**, **1**, **2** and **3**

	1	**2**	**3(A)**	**3(B)**	**L2** [a]
Bond lengths					
Br1–C7	1.92(2)	1.895(5)	1.86(2)	1.90(2)	1.901(6)
N1–C2	1.35(2)	1.367(6)	1.36(3)	1.28(3)	1.366(6)
C2–C3	1.45(2)	1.524(7)	1.48(3)	1.52(3)	1.512(8)
C3–N4	1.47(2)	1.486(7)	1.50(3)	1.57(3)	1.457(7)
N4–C5	1.23(2)	1.297(6)	1.24(2)	1.23(3)	1.274(6)
C5–C51	1.50(2)	1.472(7)	1.48(3)	1.45(3)	1.465(6)
C51–C91	1.38(2)	1.394(7)	1.37(3)	1.45(3)	1.404(8)
N1–C10	1.46(2)	1.471(6)	1.48(3)	1.49(3)	1.471(9)
C2–O11	1.28(2)	1.220(6)	1.29(3)	1.22(3)	1.211(6)
C3–C12	1.49(2)	1.511(7)	1.47(3)	1.58(4)	1.510(7)
C5–C1′ [b]	1.50(3)	1.472(7)	1.55(3)	1.61(3)	1.506(8)
Bond angles					
N1–C2–C3	121.2(16)	119.8(4)	118.5(19)	116.0(19)	115.7(4)
C2–C3–N4	107.4(14)	110.2(4)	106.0(19)	110.2(18)	108.0(4)
C3–N4–C5	122.6(14)	120.9(4)	114.4(16)	115.3(19)	118.1(4)
N4–C5–C51	122.4(15)	124.4(5)	125.4(18)	128.0(19)	124.4(5)
C5–C51–C91	118.3(14)	121.6(4)	120.5(17)	124.0(19)	122.4(4)
C51–C91–N1	125.0(15)	122.0(4)	121.4(18)	116.7(19)	121.9(4)
C91–N1–C2	118.9(14)	125.3(4)	116.9(18)	126.0(19)	123.8(4)
Torsion angles					
C2–N1–C91–C51	−53(2)	44.6(7)	58(3)	57(3)	−45.6(7)
N4–C5–C51–C91	45(2)	−50.4(7)	−44(3)	−37(4)	42.2(8)
C91–N1–C2–C3	13(2)	−12.4(7)	−12(3)	−14(3)	5.0(7)
C3–N4–C5–C51	−2(2)	6.0(6)	2(3)	1(3)	1.1(8)
N1–C2–C3–N4	61(2)	−57.7(6)	−70(2)	−66(2)	70.2(5)
C5–N4–C3–C2	−69(2)	62.4(5)	74(2)	69(2)	−74.1(6)

[a] Geometric parameters of the structure of **L2** are taken from our previous paper [19].
[b] C1′ is a pyridyl C-atom bonded to the C5 of a diazepine ring (C14 in **1** and **2**, C17 in **L2** and **3**).

Table 3
Bond lengths (Å) and angles (°) in the M^{II} coordination spheres of **1**, **2** and **3**

	1	**2**	**3(A)**	**3(B)**
Bond lengths				
M–Cl1	2.255(5)	2.2788(14)	2.183(7)	2.180(9)
M–Cl2	2.211(6)	2.2905(14)	2.191(8)	2.23(1)
M–N4	2.11(1)	2.027(4)	2.09(2)	2.11(2)
M–N2′ [a]	2.17(2)	2.004(3)	2.08(2)	2.03(2)
M–O13	2.22(1)			
Bond angles				
Cl1–M–Cl2	119.0(2)	90.50(4)	121.2(3)	115.4(4)
Cl1–M–N4	122.0(4)	95.42(11)	125.3(5)	112.3(6)
Cl1–M–N2′	94.6(4)	174.25(10)	108.9(5)	119.9(6)
Cl1–M–O13	94.2(3)			
Cl2–M–N4	118.7(4)	174.08(11)	103.9(5)	125.2(6)
Cl2–M–N2′	106.0(4)	94.12(10)	110.2(5)	101.1(7)
Cl2–M–O13	98.3(3)			
N4–M–N2′	74.3(5)	79.97(14)	79.1(7)	76.5(8)
N4–M–O13	73.0(5)			
N2′–M–O13	145.8(5)			

[a] N2′ is a pyridyl nitrogen (N15 in **1** and **2**, N18 in **3**).

containing enzymes, Zn^{II} is mostly four-coordinated [33].

The crystal structure of **1** is characterised by the hydrogen bond O13–H···O20 which connects the complex with ethanol as the solvent molecule. In the crystal structure of **2**, two equally populated positions of the hydrogen atom at O13 were observed. As a consequence of this structural disorder, O13 is (as a donor) involved in two different hydrogen bonds; with the carbonyl oxygen of the solvent molecule and with the bromine from a neighbouring molecule (Table 4, Fig. 4). In the crystal structure of **3** only weak van der Waals interactions were observed.

3.3. Infrared spectra

The IR spectra of the free benzodiazepine ligands and their complexes are complicated with significant vibrational coupling and overlapping of absorption bands. Upon metal coordination, the marked changes of ligand bands may be noticed between 1700 and 1500 cm^{-1} where the azomethine and pyridine C=N, lactam and acetate C=O, and aromatic C=C stretching vibrations are found [19,34]. In the spectra of complexes with *N*,*N*-chelatation (complexes **2**, **3** and **4**), most of these bands are shifted to lower frequencies, while in Zn^{II} complex **1** in which **L1** acts as a *N*,*N*,*O*-tridentate ligand, they are

Table 4
Hydrogen bonds in complexes **1** and **2**

	D–H···*A* (Å)	D–H (Å)	H···*A* (Å)	D–H···*A* (°)	Symmetry operation on *A*
1					
O13–H···O20	2.71	1.12	1.63	162	$-x, y-0.5, 0.5-z$
2					
O13–H···O31	2.628	0.84	1.79	172	
O13–H···Br	3.060	0.80	2.30	160	$-x, 0.5+y, 0.5-z$

shifted slightly to the higher frequency region. The similar spectral pattern was observed in the Cu^{II} complex of this ligand with the similar fivefold metal–ligand coordination [19].

The far-IR spectra (400–200 cm^{-1}) of complexes give insight into the metal–ligand vibrations. In complex **1**, a very broad band of weak to medium intensity between 350 and 240 cm^{-1} covers the whole region expected for stretching modes of the zinc–oxygen/halogen/nitrogen vibrations for this kind of complex [35,36]. The absence of highly characterised zinc-specific vibrations may be ascribed to low symmetry of this complex and to the presence of a mixture of conformers. A complicated spectral pattern was found also in **3** and **4**, where the internal deformation modes of the acetate ligand are superimposed on the metal–ligand vibrations. The spectrum of **2** shows four rather sharp bands in this frequency region, as expected for the *N*,*N*-bonded dichloro *cis*-square-planar Pd^{II} complexes [22].

3.4. ^1H NMR spectra

The ^1H NMR data of the free ligands **L1** and **L2**, their Zn^{II} complexes in $CDCl_3$ and Pd^{II} complexes in DMSO-d_6, are summarised in Table 5 according to the numbering scheme shown in Scheme 1. The spectral studies have shown that Pd^{II} complexes retain their integrity in DMSO solution, while this solvent with strong complexing ability initiates dissociation of Zn^{II} complexes by displacing the benzodiazepine ligands. This is in accordance with the assumption that zinc complexes generally show low stability [37].

The NMR spectral patterns of the aromatic region of free ligands **L1** and **L2** are in general similar to those obtained for various benzodiazepine derivatives [25,38–41]. The 3-H proton of the heterocyclic diazepine ring in both ligands appears as a triplet, while absorptions of the 3-CH_2 and OH protons are solvent-dependent. In **L1** two non-equivalent diastereotopic methylene protons in DMSO-d_6 give two separated multiplets due to geminal coupling and couplings with H-3 and OH protons, while two broad singlets (partly split) could be observed in chloroform solution. In **L2** these protons in $CDCl_3$ resonate as two distinctive doublet of doublets, while in DMSO-d_6 signals are overlapped giving a multiplet pattern. The OH signal in **L1** appears as a triplet (DMSO-d_6) or as a broad singlet ($CDCl_3$). The assignment of proton resonances was ascertained by connectivities in COSY spectra. The *N*,*N*-metal bonding in all the complexes through the azomethine and pyridine nitrogens brings about similar spectral changes for the aromatic protons. The pyridine protons, apart from H-3′, show a downfield shift (0.30–0.70 ppm), which may be related to the deshielding effect of the metal atom due to its magnetic anisotropy and to the lowering in the electron density in this aromatic ring following the electron-withdrawing effect of complexation. The upfield shift of H-3′ comes from two opposite phenomena, a downfield shift produced by the metal inductive effect and a prevalent upfield shift produced by the disappearance of the N-4 paramagnetic effect upon complexation [27,29]. The same two effects may also be expected to influence the H-6′ signal, but due to closer proximity of this proton to the metal, the latter effect is predominant. This situation could be explained by the fact that free ligands are characterised by *anti* orientation of the nitrogen atoms N-1′ and N-4, as two centres of high electron density, while in complexes the α-diimine system is in the *syn* orientation due to *N*,*N*-bidentate ligand coordination. For this reason, great changes could also be observed in absorptions of the H-3 and 3-CH_2 protons (Fig. 5). In complex **1**, a downfield shift of OH ($\sim$1 ppm) and 3-CH_2 ($\sim$3 ppm) signals supports the ligand coordination also through the hydroxy oxygen (Fig. 1). The absorption of the H-3 proton with a downfield shift ($\sim$0.40 ppm) and that of OH with an upfield shift ($\sim$0.70 ppm) are overlapped in complex **2**, giving a very broad signal at about 4 ppm. Not visible is the coupling with the adjacent 3-CH_2 protons, which appeared as two separate singlets with downfield shifts of approximately 1.35 ppm with respect to the free ligand. The second set of signals observed for the pyridine H-3′ and H-6′ protons (in a ratio $\sim$1:8) may be ascribed to the presence of two isomeric forms caused by restricted rotation within the Pd^{II} coordination sphere. In complexes **3** and **4**, the H-3 proton shows a downfield shift of 0.32 and 2.14 ppm, respectively. There are also differences in the 3-CH_2 resonances. In **4**, signals of diastereotopic methylene protons show upfield shifts of 0.78 and 0.98 ppm, while in **3** one of them

Table 5
^{1}H NMR spectral data [a]

Compound Solvent Proton	**L1** $CDCl_3$	**1** $CDCl_3$	**L1** DMSO-d_6	**2** DMSO-d_6	**L2** $CDCl_3$	**3** $CDCl_3$	**L2** DMSO-d_6	**4** $CDCl_3$
N–CH_3	3.41 (s)	3.46 (s)	3.27 (s)	3.31 (s)	3.42 (s)	3.43 (s)	3.29 (s)	3.28 (s)
H-3	3.83 (t) $^3J_{HH}$ = 7.2 Hz	4.23 (t) $^3J_{HH}$ = 5.9 Hz	3.63 (t) $^3J_{HH}$ = 6.3 Hz	3.95 [b]	3.95 (t) $^3J_{HH}$ = 6.5 Hz	4.27 (t) $^3J_{HH}$ = 4.3 Hz	3.95 (t) $^3J_{HH}$ = 6.3 Hz	6.09 (t) $^3J_{HH}$ = 6.5 Hz
3-CH_2	4.21, 4.44 (2 br s)	7.54; 7.72 (2 dd) $^3J_{HH}$ = 6.5 Hz J_{gem} = 9.8 Hz	3.97, 4.15 (2 m)	5.33, 5.80 (2 s)	4.83, 4.96 (2 dd) $^3J_{HH}$ = 6.6 Hz J_{gem} = 11.2 Hz	4.72, 5.14 (2 dd) $^3J_{HH}$ = 4.4 Hz J_{gem} = 12.2 Hz	4.63 (m) [c]	3.65, 3.85 (2 dd) $^3J_{HH}$ = 6.6 Hz J_{gem} = 11.6 Hz
OH (3b) [d]	3.02 br s	4.03 br s	4.71 t $^3J_{HH}$ = 5.4 Hz	~4.0 (br s) [e]				
$COCH_3$					2.08 (s)	2.36 (s)	1.99 (s)	1.94 (s)
H-6	7.52 (d) $^4J_{HH}$ = 2.1 Hz	7.88 (d) $^4J_{HH}$ = 2.2 Hz	7.53 (d) $^4J_{HH}$ = 2.0 Hz	8.00 (s)	7.55 (d) $^4J_{HH}$ = 2.2 Hz	7.80 (d) $^4J_{HH}$ = 2.2 Hz	7.53 (s)	7.95 (d) $^4J_{HH}$ = 2.1 Hz
H-8	7.66 (dd) $^3J_{HH}$ = 8.5 Hz $^4J_{HH}$ = 2.1 Hz	7.92 (dd) $^3J_{HH}$ = 8.8 Hz $^4J_{HH}$ = 2.4 Hz	7.79 (dd) $^3J_{HH}$ = 8.8 Hz $^4J_{HH}$ = 2.0 Hz	7.98 [f]	7.67 (dd) $^3J_{HH}$ = 8.8 Hz $^4J_{HH}$ = 2.5 Hz	7.95 (dd) $^3J_{HH}$ = 8.7 Hz $^4J_{HH}$ = 2.1 Hz	7.81 (dd) $^3J_{HH}$ = 8.6 Hz $^4J_{HH}$ = 2.0 Hz	8.01 (dd) $^3J_{HH}$ = 9.0 Hz $^4J_{HH}$ = 2.0 Hz
H-9	7.24 (d) $^3J_{HH}$ = 8.5 Hz	7.44 (d) $^3J_{HH}$ = 8.8 Hz	7.51 [g]	7.58 (d) $^3J_{HH}$ = 9.2 Hz	7.27 (d) $^3J_{HH}$ = 8.8 Hz	7.43 (d) $^3J_{HH}$ = 9.1 Hz	7.53 (d) $^3J_{HH}$ = 8.4 Hz	7.57 (d) $^3J_{HH}$ = 9.0 Hz
H-3′	8.14 (d) $^3J_{HH}$ = 7.5 Hz	7.89 [h]	8.13 (d) $^3J_{HH}$ = 7.5 Hz	7.87 (7.78) (d) [i] $^3J_{HH}$ = 8.1 Hz	8.18 (d) $^3J_{HH}$ = 7.9 Hz	7.88 [c]	8.06 (d) $^3J_{HH}$ = 8.0 Hz	7.79 (d) $^3J_{HH}$ = 7.7 Hz
H-4′	7.83 (td) $^3J_{HH}$ = 7.5 Hz $^4J_{HH}$ = 1.1 Hz	8.13 (td) $^3J_{HH}$ = 8.0 Hz $^4J_{HH}$ = 1.5 Hz	7.93 (t) $^3J_{HH}$ = 7.6 Hz	8.34 (t) $^3J_{HH}$ = 8.0 Hz	7.86 (td) $^3J_{HH}$ = 7.8 Hz $^4J_{HH}$ = 1.5 Hz	8.22 (t) $^3J_{HH}$ = 8.1 Hz	7.95 (t) $^3J_{HH}$ = 7.6 Hz	8.30 (t) $^3J_{HH}$ = 7.5 Hz
H-5′	7.40 (ddd) $^3J_{HH}$ = 7.5 Hz $^3J_{HH}$ = 4.5 Hz $^4J_{HH}$ = 1.1 Hz	7.81 (dd) $^3J_{HH}$ = 7.3 Hz $^3J_{HH}$ = 5.4 Hz	7.49 [j]	7.96 [k]	7.41 (t) $^3J_{HH}$ = 6.9 Hz	7.90 [l]	7.51 [m]	7.92 (t) [h] $^3J_{HH}$ = 7.3 Hz
H-6′	8.64 (d) $^3J_{HH}$ = 4.5 Hz	9.02 (d) $^3J_{HH}$ = 4.4 Hz	8.53 (d) $^3J_{HH}$ = 4.2 Hz	9.23 (9.15) (d) [i] $^3J_{HH}$ = 5.7 Hz	8.64 (d) $^3J_{HH}$ = 4.2 Hz	8.98 (d) $^3J_{HH}$ = 4.1 Hz	8.57 (d) $^3J_{HH}$ = 4.7 Hz	9.14 (d) $^3J_{HH}$ = 5.3 Hz

[a] Chemical shifts in ppm relative to TMS coupling constants in Hz. Multiplicities: s, singlet; d, doublet; dd, doublet of doublet; t, triplet; m, multiplet; br, broad signal.
[b] Overlapped with OH. Tentative value obtained from a ^{1}H–^{1}H COSY experiment.
[c] Visible as a sextet with $J(H^3H^{3a}) \sim 6.3$ and $J_{gem} \sim 12$ Hz.
[d] D_2O exchangeable proton.
[e] Overlapped with H-3.
[f] Partly overlapped with H-5′. Tentative value obtained from a COSY experiment.
[g] Overlapped with H-5′ and H-6. Tentative value obtained from a COSY experiment.
[h] Partly overlapped with H-6. Tentative value obtained from a COSY experiment.
[i] Value for the minor isomer is given in parenthesis.
[j] Partly overlapped with H-9. Tentative value obtained from a COSY experiment.
[k] Partly overlapped with H-6 and H-8. Tentative value obtained from a COSY experiment.
[l] Partly overlapped with H-3′. Tentative value obtained from a COSY experiment.
[m] Overlapped with H-6 and H-9. Tentative value obtained from a COSY experiment.

shows a slight downfield shift and the second one a slight upfield shift. In both complexes the separation between the two sets of signals becomes larger (up to 0.30 ppm) than in free ligand **L2**. This variation in spectral patterns of methylene protons indicates their different proximity to the metal centre. The proton chemical shifts of the remote $N–CH_3$ and $COCH_3$ groups, as well as of H-8 and H-9 of the second aromatic ring, are practically unchanged in comparison to the free ligands. The H-6 proton shows a downfield shift of 0.25–0.47 ppm.

3.5. In vitro cytostatic activity

The cytostatic activity of the free benzodiazepine ligands **L1** and **L2** and their Zn^{II}, Pd^{II} and Cu^{II} complexes was determined in vitro against the murine leukemia L1210/0 cell line as well as the human T-lymphoblast Molt4/C8 and CEM/0 cell lines. The data, expressed as concentration of the compound required to inhibit tumour cell growth by 50% (IC_{50}), are summarised in Table 6. None of the examined compounds were found to exhibit cytostatic activity at therapeutically meaningful concentrations (1–10 μg ml^{-1}). Their activity varied widely from 40 to >500 μg ml^{-1}, and the most active is the Pd^{II} complex **2** with IC_{50} values within 40–60 μg ml^{-1}. There were no significant differences in response between the three cell lines used.

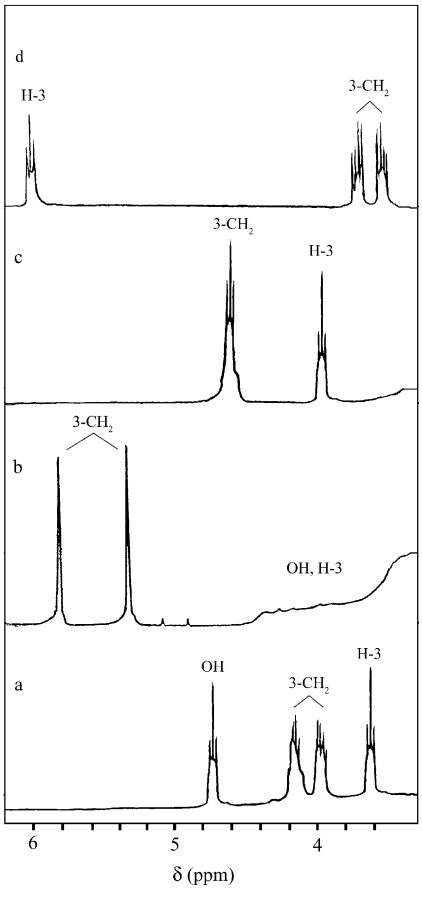

Fig. 5. Selected portions of ^1H NMR spectra of **L1** (a), **2** (b), **L2** (c) and **4** (d).

Table 6
In vitro cytostatic activity of **L1** and **L2** and their Zn^{II}, Pd^{II} and Cu^{II} complexes

Compound	IC_{50} (μg l^{-1}) [a]		
	L1210/0 [b]	Molt4/C8 [c]	CEM/0 [c]
L1	430±100	384±116	>500
1	194±40	168±19	213±6
2	44±5	51±15	45±7
Cu**L1**Cl_2	220±5	174±3	190±6
L2	90±38	51±10	51±4
3	206±5	164±9	208±9
4	210±37	154±82	169±18
Cu**L2**Cl_2	102±82	86±44	49±6

[a] 50% inhibitory concentration.
[b] L1210 murine leukemia cell line.
[c] Molt4/C8 and CEM/0-human T-lymphoblast cell lines.

3.6. In vitro antiviral activity

The antiviral assays of free benzodiazepine ligands and their complexes were based on an inhibition of virus-induced cytopathogenicity in Vero, HEL or HeLa cell cultures against a variety of DNA and RNA viruses. The antiviral activity expressed as concentration of the compound required to reduce virus-induced cytopathogenicity by 50% as well as their cytotoxicity expressed as a concentration of the compound required to cause a microscopically detectable alteration of normal cell morphology, obtained in Vero cell cultures are summarised in Table 7, together with bromovinyldeoxyuridine (BVDU), (*S*)-9-(2,3-dihydroxypropyl)adenine [(*S*)-DHPA] and ribavirin as the control test compounds. The results obtained in HEL and HeLa cells are given as Supplementary Material available from the authors upon request. The compounds showed no or only marginal antiviral activity. No antiviral effects were noted for any of the compounds against any of the viruses evaluated at concentrations that were at least fivefold below the cytotoxic concentrations. The latter ranged from 40 to 200 μg ml^{-1}.

4. Supplementary material

Crystallographic data for the structures reported in this paper have been deposited with the Cambridge Crystallographic Data Centre, CCDC Nos. 177526–177528 for compounds **1**, **3**, **2**. Copies of the data may be obtained free of charge on application to The Director, CCDC, 12 Union Road, Cambridge, CB2

Table 7
In vitro cytotoxicity and antiviral activity of **L1** and **L2** and their Zn^{II}, Pd^{II} and Cu^{II} complexes in Vero cell cultures

Compound	Minimum cytotoxic concentration (μg ml^{-1}) [a]	Minimum inhibitory concentration (μg ml^{-1}) [b]				
		Parainfluenza-3 virus	Reovirus-1	Sindbis	Coxsackie virus B4	Punta toro virus
L1	≥ 200	> 200	> 200	> 200	> 200	> 200
1	200	> 40	> 40	> 40	> 40	> 40
2	≥ 40	> 40	> 40	> 40	> 40	> 40
Cu**L1**Cl_2	200	> 40	> 40	> 40	> 40	> 40
L2	200	> 40	> 40	> 40	> 40	> 40
3	200	> 40	> 40	> 40	> 40	> 40
4	≥ 40	> 40	> 40	> 40	> 40	> 40
Cu**L2**Cl_2	200	> 40	> 40	> 40	> 40	> 40
BVDU	> 400	> 400	> 400	> 400	> 400	> 400
(*S*)-DHPA	> 400	80	240	> 400	> 400	> 400
Ribavirin	> 400	48	48	> 400	> 400	48

[a] Required to cause a microscopically detectable alteration of normal cell morphology.
[b] Required to reduce virus-induced cytopathogenicity by 50%.

1EZ, UK (fax: +44-1223-336033; e-mail: deposit@ccdc.cam.ac.uk or www: http://www.ccdc.cam.ac.uk).

Acknowledgements

This work was kindly supported by the grants 0098035, 0098036 and 0098050 from the Ministry of science and technology of the Republic of Croatia. The authors also thank Dr Bram Schierbeck, Bruker Nonius, Delft, The Netherlands, for the data collection of compound **1**.

References

[1] H.J. Roth, A. Kleemann, T. Besswenger, Pharmaceutical Chemistry, vol. 1, Wiley, New York, 1997, pp. 312–323.
[2] N.E. Kohl, S.C. Mosser, S.J. deSolms, E.A. Giuliani, D.L. Pompliano, S.L. Graham, R.L. Smith, E.M. Scolnick, A. Oliff, J.B. Gibbs, Science 260 (1993) 1934.
[3] R.F. Squires, C. Braestrup, Nature 266 (1977) 732.
[4] H. Mohler, T. Okada, Science 198 (1977) 849.
[5] C. Braestrup, R.F. Squires, Proc. Natl. Acad. Sci. USA 74 (1977) 3805.
[6] D. Hadjipavlou-Litina, C. Hansch, Chem. Rev. 94 (1994) 1483.
[7] N. Langlois, A. Rojas-Rousseau, C. Gaspard, G.H. Werner, F. Darro, R. Kiss, J. Med. Chem. 44 (2001) 3754.
[8] E. De Clercq, Actual. Chim. Thér. 18 (1991) 133.
[9] I.A. O'Neal, C.L. Murray, R.C. Hunter, S.B. Kalindjian, T.C. Jenkins, Synlett (1997) 78.
[10] A. Marchi, L. Marvelli, R. Rossi, V. Bertolasi, V. Ferretti, Inorg. Chim. Acta 272 (1998) 267.
[11] M.C. Aversa, P. Giannetto, G. Bruno, M. Cusumano, A. Giannetto, S. Geremia, J. Chem. Soc., Dalton Trans. (1990) 2433.
[12] P. Bombicz, E. Forizs, J. Madarasz, A. Deak, A. Kalman, Inorg. Chim. Acta 315 (2001) 229 (and the references therein).
[13] A. Avdagić, V. Šunjić, Helv. Chim. Acta 81 (1998) 85.
[14] P. Čudić, B. Klaić, Z. Raza, D. Šepac, V. Šunjic, Tetrahedron 47 (1991) 5295.
[15] M. Majerić-Elenkov, D. Žiher, A. Višnjevac, Z. Hameršak, B. Kojić-Prodić, V. Šunjić, Croat. Chem. Acta 74 (2001) 707.
[16] A. Avdagić, A. Lesac, Z. Majer, M. Hollosi, V. Šunjić, Helv. Chim. Acta 81 (1998) 1567.
[17] V. Vinković, Z. Raza, V. Šunjić, Spectrosc. Lett. 27 (1994) 269.
[18] E. Decorte, R. Toso, A. Šega, V. Šunjić, Ž. Ružić-Toroš, B. Kojić-Prodić, Helv. Chim. Acta 64 (1981) 1145.
[19] A. Višnjevac, Lj. Tušek-Bozić, M. Majerić-Elenkov, V. Šunjić, B. Kojić-Prodić, Eur. J. Inorg. Chem. (2001) 2647.
[20] L. Spek, HELENA, Program for Data Reduction, University of Utrecht, Utrecht, The Netherlands, 1993.
[21] A. Altomare[1], G. Cascarano[1], C. Giacovazzo[1], A. Guagliardi[1], A.G.G. Moliterni[1], M.C. Burla[2], G. Polidori[2], M. Camalli[3], R. Spagna[3], SIR-97: A Package for Crystal Structure Solution by Direct Methods and Refinement, [1]Istituto di Ricerca per lo Sviluppo di Metodologie Cristallografiche, Bari, [2]Dipartimento di Scienze della Terra, Perugia, [3]Istituto di Strutturistica Chimica 'G. Giacomello', Roma, Italy, 1997.
[22] G.M. Sheldrick, SHELXS-86: Program for the Solution of Crystal Structures, Universität Göttingen, Germany, 1986.
[23] H.D. Flack, G. Bernardinelli, J. Appl. Crystallogr. 11 (2000) 43.
[24] G.M. Sheldrick, SHELX-97: Program for the Refinement of Crystal Structures, Universität Göttingen, Germany, 1997.
[25] T. Spek, PLATON-98: A Multipurpose Crystallographic Tool, 120398 Version, University of Utrecht, Utrecht, The Netherlands, 1998.
[26] E. De Clercq, J. Balzarini, P.F. Torrence, M.P. Mertes, C.L. Schmidt, D. Shugar, P.J. Barr, A.S. Jones, G. Verhelst, R.T. Walker, Mol. Pharmacol. 19 (1981) 321.
[27] Lj. Tušek-Bozić, A. Furlani, V. Scarcia, E. De Clercq, J. Balzarini, J. Inorg. Biochem. 72 (1998) 201.
[28] E. De Clercq, In vitro and ex vivo test systems to rationalize drug design and delivery, in: D. Crommelin, P. Couvreur, D. Duchene (Eds.), Editions de Santé, Paris, France, 1994, pp. 108–125.
[29] C.K. Johnson, ORTEP-II, Report ORNL-5138, Oak Ridge National Laboratory, TN, 1976.
[30] F.H. Allen, O. Kennard, Chem. Des. Automation News 8 (1993) 1.
[31] A. Višnjevac, Stereochemistry of the chiral 1,4-benzodiazepin-2-ones and their metal complexes, PhD Thesis, University of Zagreb, Zagreb, Croatia, 2001.
[32] G. Parkin, Chem. Commun. 20 (2000) 1971.
[33] I.L. Alberts, K. Nadassy, S.J. Wodak, Protein Sci. 7 (1998) 1700.
[34] M.A. Cinellu, M.L. Ganadu, G. Minghetti, F. Cariati, F. Demartin, M. Manassero, Inorg. Chim. Acta 143 (1988) 197.

[35] K. Nakamoto, Infrared and Raman Spectra of Inorganic and Coordination Compounds, Part B: Applications in Coordination, Organometallic and Bioinorganic Chemistry, 5th ed., Willey-Interscience, New York, 1997, pp. 24 and 59.
[36] S. Gourbatsis, S.P. Perlepes, J.S. Butler, N. Hadjiliadis, Polyhedron 18 (1999) 2369.
[37] A. Abufarag, H. Vahrenkamp, Inorg. Chem. 34 (1995) 2207.
[38] M.C. Aversa, P. Bonaccorsi, M. Cusumano, P. Gianneto, D. Minniti, J. Chem. Soc., Dalton Trans. (1991) 3431.
[39] S. Stoccoro, M.A. Cinellu, A. Zucca, G. Minghetti, Inorg. Chim. Acta 215 (1994) 17.
[40] M. Cusumano, A. Giannetto, D. Minniti, Inorg. Chim. Acta 215 (1994) 41.
[41] M.J. Mphahlele, P. Kaye, Magn. Reson. Chem. 38 (2000) 207.